Fast neutrino-flavor swap in high-energy astrophysical environments

Masamichi Zaizen*
Faculty of Science and Engineering, Waseda University, Tokyo 169-8555, Japan

Hiroki Nagakura
Division of Science, National Astronomical Observatory of Japan, 2-21-1 Osawa, Mitaka, Tokyo 181-8588, Japan

(Received 27 November 2023; accepted 29 March 2024; published 25 April 2024)

We assert that nonlinear features of fast neutrino-flavor conversion (FFC) can be qualitatively different between core-collapse supernovae (CCSNe) and binary neutron star mergers (BNSMs). This argument arises from recent global FFC simulations in BNSM, in which fast flavor swap (FFS) emerges in very narrow spatial regions, whereas neutrinos in CCSN tend to evolve toward flavor equipartition. In this paper, we provide the physical mechanism of FFS based on a colliding neutrino beam model. Neutrinos/antineutrinos can undergo FFS when they propagate in ambient neutrino gas that propagates in the opposite direction and also has the opposite sign of ELN-XLN, where ELN and XLN denote electron- and heavy-leptonic neutrino number, respectively. Such environments can be naturally realized in BNSMs, whereas they are unlikely in CCSNe unless the neutrino sphere is strongly deformed aspherically. Our study exhibits the diversity of nonlinear dynamics of FFC.

DOI: 10.1103/PhysRevD.109.083031

I. INTRODUCTION

Neutrino flavor evolution plays important roles in the dynamics of core-collapse supernovae (CCSNe) and binary neutron star mergers (BNSMs). During the last decade, their numerical models with classical neutrino transport schemes have cultivated our understandings of complex physical processes including weak interactions, gravity, and equation of states [1–5]. Meanwhile, recent progress in neutrino quantum kinetics has indicated that flavor conversion driven by neutrino self-interactions can bring significant change in the neutrino radiation field [6–9].

Fast neutrino-flavor conversion (FFC), which is induced by a zero crossing in ELN (electron neutrino-lepton number)-XLN (heavy-leptonic one) angular distributions, has particularly received significant attention. This phenomenon induces *pairwise* flavor conversion, $\nu_e\bar{\nu}_e \leftrightarrow \nu_x\bar{\nu}_x$ (ν_e and $\bar{\nu}_e$ represent electron-type neutrinos and their antipartners, respectively; x denotes heavy-leptonic flavors, μ or τ), conserving the net flavor distribution. Linear stability analyses of flavor instabilities have been carried out for CCSN/BNSM models, and these studies have revealed that FFC occurs in both CCSNe [10–18] and BNSMs [19–25]. It should be noted, however, that we still have little knowledge concerning how the neutrino radiation field is actually changed after FFC grows substantially. This indicates that the impacts of FFC on CCSN/BNSM remain a matter of debate [6,26–29].

It has also been suggested that flavor mixing occurring in their environments is not only FFC but also collision-induced one, so-called collisional flavor instability (CFI) [30], and matter-neutrino resonance (MNR) [31]. The former is driven by the disparity in the neutrino reaction rates with matter between neutrinos and antineutrinos. The possibility in BNSMs [32] and CCSNe [33,34] has been discussed based on the linear stability analysis, and the nonlinear behaviors have been also investigated [8,35–37]. These studies showed that CFI can occur in the deeper neutrino-opaque region than FFC, indicating that they can also be a potential game-changer for BNSMs and CCSNe.

It should be mentioned that the latter (MNR) can occur in BNSMs [31,38–45], but it is unlikely in CCSN environments. This is because the electron-lepton number is always positive in CCSNe, which suppresses the MNR. On the other hand, the number density of $\bar{\nu}_e$ can dominate over ν_e in some regions, which yields negative strength of neutrino self-interaction potential. This can cancel the positive matter potential, which potentially induce MNR. Although it is an intriguing question how these flavor conversion impact on fluid dynamics and nucleosynthesis in BNSMs, the detailed studies are postponed to another paper and we focus only on FFC in the present study.

CCSNe and BNSMs are attractive sites exhibiting rich flavor conversion phenomena, and the identification of the asymptotic states helps us to understand the impact on

*zaizen@heap.phys.waseda.ac.jp

them. Asymptotic states of FFCs are dictated by the interplay between neutrino advection and ELN-XLN angular distributions, where ELN and XLN represent $\nu_e - \bar{\nu}_e$ and $\nu_x - \bar{\nu}_x$, respectively. Previous local FFC simulations suggested that ELN becomes nearly equal to XLN in some angular regions, i.e., flavor equipartition so that ELN-XLN angular crossings disappear [46–50]. This can be understood analytically [50–52], and large-scale FFC simulations in spherical symmetry also support the argument [53,54]. The trend holds even in cases with including neutrino-matter interactions under realistic CCSN fluid profiles [6,29].

However, our large-scale FFC simulations in BNSM showed that the nonlinear evolution of FFC is qualitatively different from those in CCSNe [9]. Instead of balancing between ELN and XLN, FFC can proceed beyond the flavor equilibrium states, and the neutrinos eventually achieve flavor swap, i.e., complete interchange between different flavors. However, the physical mechanism of fast neutrino-flavor swap (FFS) remains entirely unknown and even unexplored yet.

In this paper, we provide the principle mechanism of FFS with performing local FFC simulations. As shall be discussed below, FFS can commonly occur in BNSM, but it seems unlikely in CCSN unless neutrino radiation fields become strongly aspherical. The present study contributes to a comprehensive understanding of asymptotic states of FFC in CCSNe and BNSMs.

II. COLLIDING NEUTRINO BEAM MODEL

We show that essential features of FFS can be demonstrated by a simple model, namely *colliding neutrino beam model*. This is a model that neutrino beams emitted at opposite boundaries collide each other. It should be mentioned that this model is different from canonical "beam" model which has been well studied in the literature [55–59]. In the canonical one, neutrino gas is assumed to be homogeneous or in the linear regime, whereas neutrino advection plays a pivotal role in our colliding beam model. Below, we present its numerical simulations, while our numerical setup is rather simple to keep our discussions as easy as possible.

The basic equation is given by quantum kinetic equation (QKE),

$$(\partial_t + v_z\partial_z)\rho(t,z,v_z) = -\mathrm{i}[H_{\nu\nu},\rho(t,z,v_z)]; \qquad (1)$$

where ρ, t, and z denote the density matrix of neutrinos, time, and space, respectively. We work in two-flavor framework and in one-dimensional (z direction) transport. We assume axial symmetry in momentum space (v_z specifies the angular point in neutrino momentum space) and also ignore the energy-dependent term such as vacuum oscillation and neutrino-matter interactions, so that we consider only energy-integrated QKEs. In this case, wave functions for anti-neutrinos can be collectively treated with those for neutrinos as negative occupations, $\bar{\rho}(E) \equiv -\rho(-E)$. The Hamiltonian of neutrino self-interactions is recast into

$$H_{\nu\nu} = \mu \int_{-1}^{+1} \mathrm{d}v_z'(1 - v_z v_z')G_{v_z'}\rho_{v_z'}, \qquad (2)$$

where $\mu = \sqrt{2}G_{\mathrm{F}}n_{\nu_e}$ and G_{v_z} is an ELN-XLN angular distribution;

$$G_v = \frac{1}{n_{\nu_e}}\int \frac{E^2\mathrm{d}E}{(2\pi)^2}[(f_{\nu_e} - f_{\nu_x}) - (f_{\bar{\nu}_e} - f_{\bar{\nu}_x})]. \qquad (3)$$

In the expression, n_{ν_η} and f_{ν_η} denote number density and distribution function of η-flavor neutrinos, respectively. Hereafter, we measure the time and space in the unit of μ^{-1} because the self-interaction potential μ is a unique dimensional quantity in the energy-integrated QKE. We cover a spatial domain of $L_z = 1000$ by a uniform spatial grid points with $N_z = 10000$ in our simulations.

As the simplest case, we inject neutrinos from each boundary as

$$G_{v_z} = 1 \quad (\text{for } v_z = 1) \qquad (4)$$

at $z = 0$ and

$$G_{v_z} = -\alpha \quad (\text{for } v_z = -1) \qquad (5)$$

at $z = L_z$, where $\alpha(> 0)$ denotes a flavor asymmetry of ELN-XLN beams between those emitted from the two boundaries. Note that $\bar{\nu}$ needs to be no longer distinguished from ν in the context of FFC. We can consider only ELN-XLN not each species, so the number density in one beam can be normalized by that in the other. During the simulation, we keep them constant in time at each boundary, while we put a small perturbation of $\sim 10^{-6}$ in the off-diagonal component of the density matrix only at $t = 0$. The negative sign of G_{v_z} for $v_z = -1$ guarantees that ELN-XLN angular crossings appear when the two beams encounter each other, marking the onset of FFC. Throughout the paper, we inject only ν_e at $z = 0$ and $\bar{\nu}_e$ at $z = L_z$ to simplify the discussion (but without any loss of generality).

Left panels in Fig. 1 show the time evolution of the survival probability of ν_e and $\bar{\nu}_e$ for $\alpha = 1$, i.e., symmetric case. As shown in the second panel from the top, FFC develops at the center of the spatial domain ($z \sim 500$) and creates a transition layer of flavor conversion there. The flavor conversions do not stop at a flavor equilibrium state, but rather, they achieve FFS ($P_{ee} \sim 0$) eventually. The neutrinos injected at $t > 0$ also undergo FFS (see from the third to fifth panels), while the transition layer is less evolved with time. In fact, P_{ee} keeps ~ 0.5 at $z = 500$ after

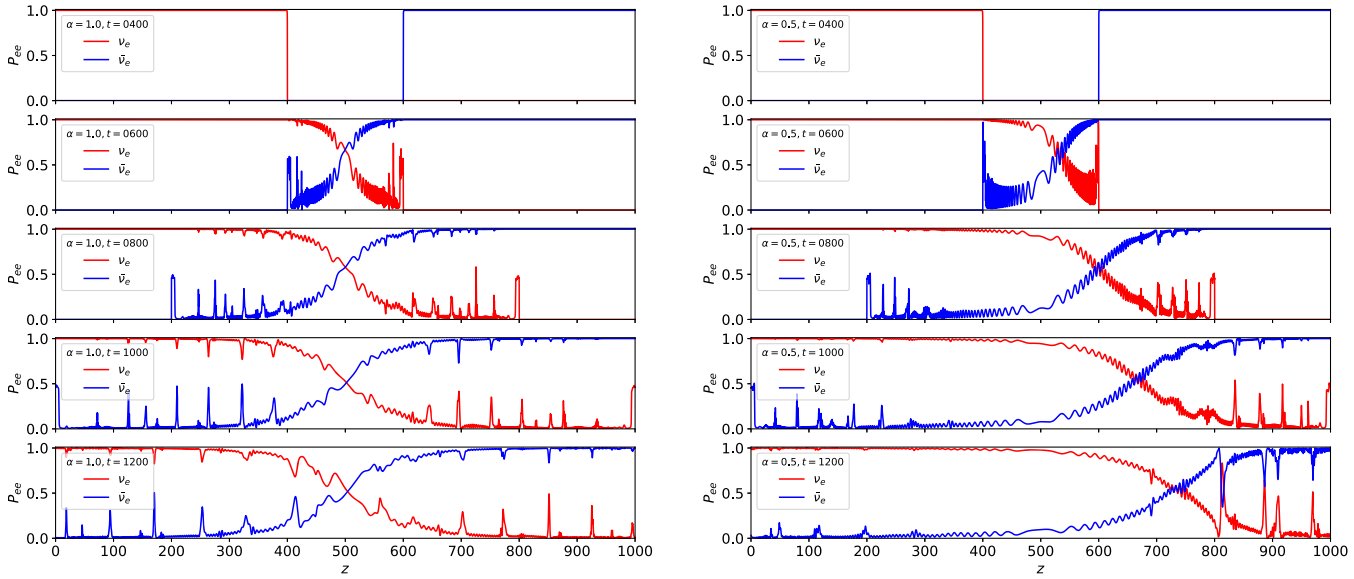

FIG. 1. Time evolution of survival probability for ν_e (red) and $\bar{\nu}_e$ (blue) in the two-beam model. Left panels show the case of $\alpha = 1$, symmetric case, and right ones the case of $\alpha = 0.5$. Transition layer moves toward positive clearly for $\alpha = 0.5$.

the two beams are colliding. This layer corresponds to ELN-XLN zero surface (EXZS), which was also observed in global FFC simulations in BNSM environment [9]. This exhibits that the colliding neutrino beam model demonstrates essentially the same phenomenon as in FFC of BNSM environments. Before we move on to the detailed discussion of the mechanism of FFS, we present some important properties of EXZS.

In the case of $\alpha = 1$, the transition layer including EXZS stagnates at $z \sim 500$. This can be naturally expected, since ν_e and $\bar{\nu}_e$ beams emitted from opposite boundaries are completely symmetric. As shown in the case with $\alpha = 0.5$ (see right panels in Fig. 1), however, the layer is no longer stationary but moves toward the positive z-direction with time. This is because the total number of neutrinos experiencing flavor conversions needs to be the same between ν_e and $\bar{\nu}_e$ in FFC. In the case of $\alpha = 0.5$, the $\bar{\nu}_e$ beam (emitted from $z = L_z$) is weaker than ν_e, indicating that the transition layer has to move with positive velocity in order to satisfy the number flux across the EXZS.

To develop the discussion more quantitatively, we show spatial distributions of P_{ee} at multiple time snapshots for cases with $\alpha = 1$, 0.5, and 0.1 in Fig. 2 (from top to bottom). In this figure, the horizontal axis (λ) corresponds to the z-axis normalized by the width between the head of ν_e beam ($\lambda = 1$) and $\bar{\nu}_e$ ($\lambda = 0$). The $\lambda-$coordinate is useful to show results at different time snapshots in the same scale. A noticeable feature appearing in Fig. 2 should be mentioned here. The transition layer (or the position of EXZS, $\lambda = \lambda_{\rm EXZS}$) is nearly time-independent in the λ-space, which reflects that the layer is determined by the conservation law of neutrinos in FFC. This is because the total ν_e that passing through $\lambda = \lambda_{\rm EXZS}$ (i.e., undergoing FFS) is $G_{v_z=1} \times (1 - \lambda_{\rm EXZS})$, while that of $\bar{\nu}_e$ is $G_{v_z=-1} \times \lambda_{\rm EXZS}$. Assuming FFS, both of them are equal to each other, leading to $\lambda_{\rm EXZS} = 1/(1+\alpha)$. This illustrates that the transition layer is constant in time in λ-space. Indeed, our numerical simulations show that EXZS is located at $\lambda_{\rm EXZS} \sim 1/(1+\alpha)$ (see dotted vertical lines in Fig. 2).

This argument for the position of EXZS in λ-space is also useful to estimate the moving velocity of EXZS in real z-space. We note that the area between the head of ν_e and $\bar{\nu}_e$ expands with time ($\Delta L_z = 2c \times \Delta t$, where ΔL_z and c denote the expansion length in the time interval of Δt and the speed of light, respectively), indicating that the EXZS

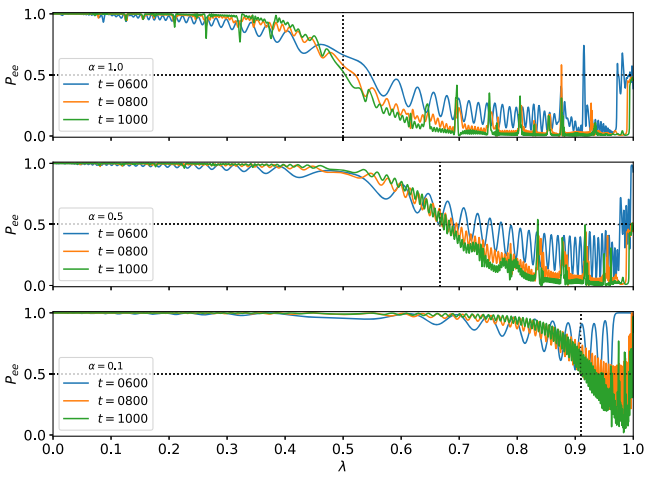

FIG. 2. Time evolution of survival probability in the domain scaled by the interval between the leading parts of injected neutrinos for $\alpha = 1$ (top), 0.5 (middle), and 0.1 (bottom). Dotted vertical line is $\lambda_{\rm EXZS}$.

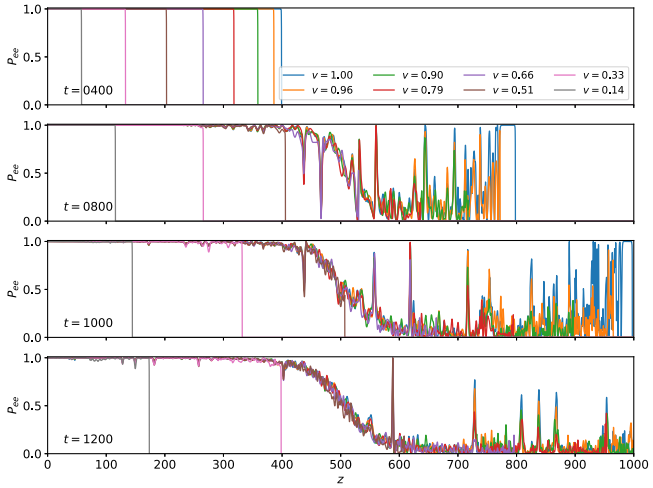

FIG. 3. Time evolution of survival probability in the multiple-beams model ($N_{v_z} = 32$) with $\alpha = 1$. The positive-velocity components are only shown.

position in z-space becomes time-dependent in general. The velocity of EXZS ($v_{\rm EXZS}$) can be estimated as,

$$v_{\rm EXZS} = 2c \times (\lambda_{\rm EXZS} - 0.5) = \frac{1-\alpha}{1+\alpha} c. \tag{6}$$

This is a rationale behind the time evolution of EXZS displayed in Fig. 1 and also those found in global FFC simulations in BNSM [9].

One may wonder if FFS occurs in multiple beams. In Fig. 3, we show time- and spatial distributions of P_{ee} for the same simulation with $\alpha = 1$ but with multiple beams ($N_{v_z} = 32$). In this simulation, we inject 16 ν_e-beams and the same number of $\bar{\nu}_e$-beams from $z = 0$ and L_z, respectively. The number density of neutrinos for each ray is assumed to be the same, while the flight direction is distributed in $0(-1) \le v_z \le 1(0)$ for $\nu_e(\bar{\nu}_e)$ according to Gauss-Legendre quadrature. In the early phase, we find that there are some quantitative differences from the case with the two colliding beams; for instance, the onset time when flavor conversion appears is delayed. This is simply because the self-interaction potential effectively becomes weaker due to the fact that relative angles between ν_e and $\bar{\nu}_e$ are narrower than the head-on collision. On the other hand, the overall property is the same in the late phase; all neutrinos passing through EXZS undergo FFS, and the EXZS stagnates stably at $z \sim 500$.

III. MECHANISM OF FLAVOR SWAP

We now turn our attention to the physical mechanism of FFS. We consider the mechanism of FFS with the expression of polarization vector of neutrinos: $\rho = {\rm Tr}\rho/2 + \boldsymbol{P}\cdot\boldsymbol{\sigma}/2$, where $\boldsymbol{\sigma}$ denotes the Pauli matrices. The third-component (hereafter denoted as P_3) represents the degree of flavor eigenstate; $P_3 = 1$ and -1 correspond to pure ν_e and ν_x states, respectively.

We first rewrite QKE for the colliding two-neutrino beam model in terms of $\boldsymbol{P}$, which can be expressed as

$$\partial_t \boldsymbol{P} + \partial_z \boldsymbol{P} = -2\mu\alpha \bar{\boldsymbol{P}} \times \boldsymbol{P}, \tag{7}$$

$$\partial_t \bar{\boldsymbol{P}} - \partial_z \bar{\boldsymbol{P}} = 2\mu \boldsymbol{P} \times \bar{\boldsymbol{P}}, \tag{8}$$

where we assume that $\boldsymbol{P}$ ($\bar{\boldsymbol{P}}$) is nontrivial only for $v_z = 1(-1)$. It should also be mentioned that the norm of $\boldsymbol{P}$ and $\bar{\boldsymbol{P}}$ are constant in time and space where they are finite because of the absence of incoherent collision terms;

$$(\partial_t + \partial_z)\|\boldsymbol{P}\|^2 = 2\boldsymbol{P}\cdot[-2\mu\alpha\bar{\boldsymbol{P}} \times \boldsymbol{P}] = 0. \tag{9}$$

For convenience, we perform a coordinate transformation: $t' = t$ and $z' = z - ct$. This corresponds to a coordinate shifting with $v_z = 1$ (we note that the coordinate bases for t' and z' are no longer orthogonal to each other). In the coordinate, Eqs. (7) and (8) can be transformed to

$$\partial_{t'} \boldsymbol{P} = -2\mu\alpha \bar{\boldsymbol{P}} \times \boldsymbol{P} \tag{10}$$

$$\partial_{t'} \bar{\boldsymbol{P}} - 2\partial_{z'} \bar{\boldsymbol{P}} = 2\mu \boldsymbol{P} \times \bar{\boldsymbol{P}}. \tag{11}$$

Then, the second time derivative of P_3 can be written as

$$\partial_{t'}^2 P_3 = -4\mu^2\alpha \left\{ \frac{1}{\mu}[(\partial_{z'}\bar{\boldsymbol{P}}) \times \boldsymbol{P}] \cdot \hat{\boldsymbol{e}}_3 + (\alpha P_3 + \bar{P}_3) - (\boldsymbol{P}\cdot\bar{\boldsymbol{P}})(P_3 + \alpha\bar{P}_3) \right\}, \tag{12}$$

where $\hat{\boldsymbol{e}}_3$ denotes the third coordinate basis in flavor space. Hereafter, let us consider the asymptotic state ($t \to \infty$) of P_3. In the colliding beam model, $\bar{\boldsymbol{P}}$ at $t \to \infty$ is given from a boundary condition: $\bar{P}_3 = 1$ and $\partial_{z'}\bar{\boldsymbol{P}} = 0$ (since we inject $\bar{\nu}_e$ at the boundary). This indicates that Eq. (12) can be approximated as,

$$\partial_{t'}^2 P_3 \sim -4\mu^2\alpha[1 - (P_3)^2], \tag{13}$$

where we use the relation $\boldsymbol{P}\cdot\bar{\boldsymbol{P}} \sim P_3$ in the asymptotic state of ν_e where $\bar{\boldsymbol{P}} = \hat{\boldsymbol{e}}_3$. This suggests that the asymptotic state of neutrinos satisfies $P_3 = 1$ or -1. However, only $P_3 = 1$ (i.e., pure ν_e state) is clearly unstable because $\partial_{t'}^2 P_3$ is always negative, implying that FFC occurs during neutrino evolution. Equation (13) also shows that the FFC cannot stop at $P_3 = 0$ (flavor equipartition), and flavor conversion proceeds until FFS is achieved ($P_3 = -1$) and the system becomes stable. It is also worthwhile to note that the same conclusion holds for $\alpha > 0$, indicating that the flavor swap eventually takes place in the presence of $\bar{\nu}_e$ (or negative ELN-XLN).

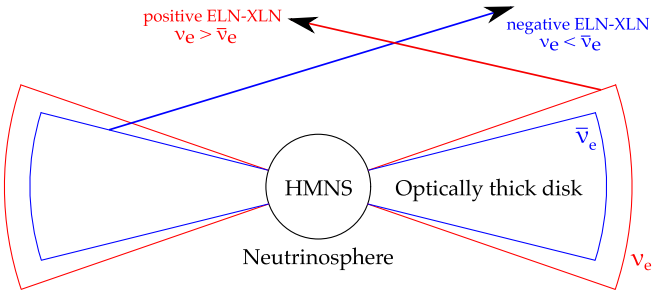

FIG. 4. Schematic pictures of neutrino rays from emission surfaces in BNSM. Neutrinos are emitted from both hypermassive neutron star (HMNS) and the surrounding disk. Shell structure in the emission surface expresses flavor-dependent neutrino sphere.

The above argument illustrates the difference from the cases where FFC achieves flavor equipartitions. In the case with flavor equipartition, both neutrinos and antineutrinos are co-evolved, indicating that the asymptotic state of $\bar{\boldsymbol{P}}$ is determined by their interplay, leading to $\bar{P}_3 \sim 0$ at the time when $\partial_{z'}\bar{P}_3 = 0$ [50–52]. In cases of colliding beam models, however, the neutrinos and antineutrinos evolve separately, and the asymptotic state of the other neutrinos/antineutrinos has already been given at the opposite boundary, which leads to FFS.

One thing we should mention is that BNSM remnants can naturally offer similar environments for occurrences of FFS. As described in Ref. [19], $\bar{\nu}_e$ usually has higher emission than ν_e, but the ν_e can dominate over $\bar{\nu}_e$ around the outer edge of ν_e sphere. This indicates that positive and negative ELN rays intersect with each other, leading to ELN angular crossings, as schematically illustrated in Fig. 4. Note that XLN is zero in the neutrino radiation field without flavor conversion. This is the similar situation in the colliding neutrino beam model, whereas it is unlikely for CCSNe to generate such globally aspherical geometry.

IV. CONCLUSIONS

In this paper, we presented the novel dynamics of fast neutrino-flavor swap (FFS), which would appear in the geometry of BNSMs. Since neutrinos in BNSMs are emitted from the surrounding disk, a broader angular distribution of neutrinos, including a nearly head-on collision, emerges and potentially has an angular crossing between ν_e and $\bar{\nu}_e$ with almost opposite characteristic velocities, whereas the environment is clearly in contrast to CCSN. Our colliding neutrino beam model captures the essential feature of such a geometry; in fact, we demonstrated FFS by the simple model. We also presented that the geometry and velocity of ELN-XLN zero surface (EXZS or a transition layer of flavor conversion) are determined so as to satisfy the conservation of the ELN-XLN number flux across the EXZS. In the domain normalized by the width between the heads of two neutrino beams, the transition layer is stationary irrespective of the flavor asymmetry while its location is given by it. This observation in our numerical results provides a rationale behind the time-dependent feature of EXZS in Ref. [9].

We also analytically showed the mechanism of FFS based on polarization vectors for neutrino density matrices. Considering the asymptotic state of ν_e, we find that FFC does not stop until the flavor swap completes. This is because $\bar{\nu}_e$ (or negative ELN-XLN), propagating in the opposite direction to ν_e, continues to be supplied from the opposite boundary. This exhibits that the occurrence of FFS hinges on the ELN-XLN distributions and the geometry of neutrino spheres, which are clearly different from the cases where FFC evolves toward flavor equipartition.

Since FFS corresponds to the most extreme case of flavor conversion, it would yield a significant change in the neutrino radiation field, particularly neutrino absorption. This affects the electron fraction of ejecta and subsequently r-process nucleosynthesis and kilonova. In CCSNe, FFS would not occur and neutrinos would achieve a flavor equipartition through normal FFC, but there is a caveat. They might occur in CCSNe if large-scale coherent asymmetric neutrino emission appears in the CCSN core. It would be realized when the CCSN core is rapidly rotating, strong lepton-number emission of self-sustained asymmetry (LESA) occurs [60–62], or the proto-neutron star is accelerated by asymmetric neutrino emission [63]. Addressing issues whether FFS can emerge in such extreme CCSN environments requires a more detailed investigation, which is deferred to our future work.

ACKNOWLEDGMENTS

We would like to express special thanks to Manu George for sharing his unpublished numerical results which inspired our colliding neutrino beam model. We are also grateful to Meng-Ru Wu, Zewei Xiong, and Lucas Johns for useful comments and discussions. We thank the Focus workshop on collective oscillations and chiral transport of neutrinos at the Academia Sinica for eliciting the discussions that led to the completion of this paper. M. Z. is supported by the Japan Society for Promotion of Science (JSPS) Grant-in-Aid for JSPS Fellows (Grants No. 22KJ2906) from the Ministry of Education, Culture, Sports, Science, and Technology (MEXT) in Japan. H. N. is supported by Grant-in-Aid for Scientific Research (23K03468). The numerical computations were carried out on Cray XC50 at the Center for Computational Astrophysics, National Astronomical Observatory of Japan. This work is also supported by HPCI System Research Project (Project ID: 230033, 230204, 230270).

[1] K. Langanke and G. Martínez-Pinedo, Nuclear weak-interaction processes in stars, Rev. Mod. Phys. **75**, 819 (2003).
[2] H.-T. Janka, Explosion mechanisms of core-collapse supernovae, Annu. Rev. Nucl. Part. Sci. **62**, 407 (2012).
[3] H.-T. Janka, Neutrino emission from supernovae, in *Handbook of Supernovae*, edited by A. W. Alsabti and P. Murdin (Springer International Publishing, Cham, 2017), pp. 1575–1604.
[4] A. Burrows and D. Vartanyan, Core-collapse supernova explosion theory, Nature (London) **589**, 29 (2021).
[5] K. Sumiyoshi, T. Kojo, and S. Furusawa, Equation of state in neutron stars and supernovae, in *Handbook of Nuclear Physics*, edited by I. Tanihata, H. Toki, and T. Kajino (Springer Nature, Singapore, 2023), pp. 1–51.
[6] H. Nagakura, Roles of fast neutrino-flavor conversion on the neutrino-heating mechanism of core-collapse supernova, Phys. Rev. Lett. **130**, 211401 (2023).
[7] S. Shalgar and I. Tamborra, Neutrino flavor conversion, advection, and collisions: Toward the full solution, Phys. Rev. D **107**, 063025 (2023).
[8] Z. Xiong, M.-R. Wu, G. Martínez-Pinedo, T. Fischer, M. George, C.-Y. Lin, and L. Johns, Evolution of collisional neutrino flavor instabilities in spherically symmetric supernova models, Phys. Rev. D **107**, 083016 (2023).
[9] H. Nagakura, Global features of fast neutrino-flavor conversion in binary neutron star mergers, Phys. Rev. D **108**, 103014 (2023).
[10] S. Abbar, H. Duan, K. Sumiyoshi, T. Takiwaki, and M. C. Volpe, On the occurrence of fast neutrino flavor conversions in multidimensional supernova models, Phys. Rev. D **100**, 043004 (2019).
[11] M. Delfan Azari, S. Yamada, T. Morinaga, H. Nagakura, S. Furusawa, A. Harada, H. Okawa, W. Iwakami, and K. Sumiyoshi, Fast collective neutrino oscillations inside the neutrino sphere in core-collapse supernovae, Phys. Rev. D **101**, 023018 (2020).
[12] H. Nagakura, T. Morinaga, C. Kato, and S. Yamada, Fast-pairwise collective neutrino oscillations associated with asymmetric neutrino emissions in core-collapse supernovae, Astrophys. J. **886**, 139 (2019).
[13] S. Abbar, H. Duan, K. Sumiyoshi, T. Takiwaki, and M. C. Volpe, Fast neutrino flavor conversion modes in multidimensional core-collapse supernova models: The role of the asymmetric neutrino distributions, Phys. Rev. D **101**, 043016 (2020).
[14] R. Glas, H.-T. Janka, F. Capozzi, M. Sen, B. Dasgupta, A. Mirizzi, and G. Sigl, Fast neutrino flavor instability in the neutron-star convection layer of three-dimensional supernova models, Phys. Rev. D **101**, 063001 (2020).
[15] T. Morinaga, H. Nagakura, C. Kato, and S. Yamada, Fast neutrino-flavor conversion in the preshock region of core-collapse supernovae, Phys. Rev. Res. **2**, 012046 (2020).
[16] H. Nagakura, A. Burrows, L. Johns, and G. M. Fuller, Where, when, and why: Occurrence of fast-pairwise collective neutrino oscillation in three-dimensional core-collapse supernova models, Phys. Rev. D **104**, 083025 (2021).
[17] A. Harada and H. Nagakura, Prospects of fast flavor neutrino conversion in rotating core-collapse supernovae, Astrophys. J. **924**, 109 (2022).
[18] R. Akaho, A. Harada, H. Nagakura, W. Iwakami, H. Okawa, S. Furusawa, H. Matsufuru, K. Sumiyoshi, and S. Yamada, Protoneutron star convection simulated with a new general relativistic Boltzmann neutrino radiation hydrodynamics code, Astrophys. J. **944**, 60 (2023).
[19] M.-R. Wu and I. Tamborra, Fast neutrino conversions: Ubiquitous in compact binary merger remnants, Phys. Rev. D **95**, 103007 (2017).
[20] M. George, M.-R. Wu, I. Tamborra, R. Ardevol-Pulpillo, and H.-T. Janka, Fast neutrino flavor conversion, ejecta properties, and nucleosynthesis in newly-formed hypermassive remnants of neutron-star mergers, Phys. Rev. D **102**, 103015 (2020).
[21] X. Li and D. M. Siegel, Neutrino fast flavor conversions in neutron-star postmerger accretion disks, Phys. Rev. Lett. **126**, 251101 (2021).
[22] S. Richers, Evaluating approximate flavor instability metrics in neutron star mergers, Phys. Rev. D **106**, 083005 (2022).
[23] O. Just, S. Abbar, M.-R. Wu, I. Tamborra, H.-T. Janka, and F. Capozzi, Fast neutrino conversion in hydrodynamic simulations of neutrino-cooled accretion disks, Phys. Rev. D **105**, 083024 (2022).
[24] E. Grohs, S. Richers, S. M. Couch, F. Foucart, J. Froustey, J. Kneller, and G. McLaughlin, Two-moment neutrino flavor transformation with applications to the fast flavor instability in neutron star mergers, Astrophys. J. **963**, 11 (2024).
[25] J. Froustey, S. Richers, E. Grohs, S. Flynn, F. Foucart, J. P. Kneller, and G. C. McLaughlin, Neutrino fast flavor oscillations with moments: Linear stability analysis and application to neutron star mergers, Phys. Rev. D **109**, 043046 (2024).
[26] S.-i. Fujimoto and H. Nagakura, Explosive nucleosynthesis with fast neutrino-flavour conversion in core-collapse supernovae, Mon. Not. R. Astron. Soc. **519**, 2623 (2023).
[27] J. Ehring, S. Abbar, H.-T. Janka, G. Raffelt, and I. Tamborra, Fast neutrino flavor conversion in core-collapse supernovae: A parametric study in 1D models, Phys. Rev. D **107**, 103034 (2023).
[28] J. Ehring, S. Abbar, H.-T. Janka, G. Raffelt, and I. Tamborra, Fast neutrino flavor conversions can help and Hinder neutrino-driven explosions, Phys. Rev. Lett. **131**, 061401 (2023).
[29] H. Nagakura and M. Zaizen, Basic characteristics of neutrino flavor conversions in the post-shock regions of core-collapse supernova, Phys. Rev. D **108**, 123003 (2023).
[30] L. Johns, Collisional flavor instabilities of supernova neutrinos, Phys. Rev. Lett. **130**, 191001 (2023).
[31] A. Malkus, A. Friedland, and G. C. McLaughlin, Matter-neutrino resonance above merging compact objects, arXiv:1403.5797.
[32] Z. Xiong, L. Johns, M.-R. Wu, and H. Duan, Collisional flavor instability in dense neutrino gases, Phys. Rev. D **108**, 083002 (2023).
[33] J. Liu, R. Akaho, A. Ito, H. Nagakura, M. Zaizen, and S. Yamada, Universality of the neutrino collisional flavor instability in core-collapse supernovae, Phys. Rev. D **108**, 123024 (2023).
[34] R. Akaho, J. Liu, H. Nagakura, M. Zaizen, and S. Yamada, Collisional and fast neutrino flavor instabilities in

two-dimensional core-collapse supernova simulation with Boltzmann neutrino transport, Phys. Rev. D **109**, 023012 (2024).
[35] Y.-C. Lin and H. Duan, Collision-induced flavor instability in dense neutrino gases with energy-dependent scattering, Phys. Rev. D **107**, 083034 (2023).
[36] J. Liu, M. Zaizen, and S. Yamada, Systematic study of the resonancelike structure in the collisional flavor instability of neutrinos, Phys. Rev. D **107**, 123011 (2023).
[37] C. Kato, H. Nagakura, and L. Johns, Collisional flavor swap with neutrino self-interactions, arXiv:2309.02619.
[38] M.-R. Wu, H. Duan, and Y.-Z. Qian, Physics of neutrino flavor transformation through matter–neutrino resonances, Phys. Lett. B **752**, 89 (2016).
[39] Y. L. Zhu, A. Perego, and G. C. McLaughlin, Matter-neutrino resonance transitions above a neutron star merger remnant, Phys. Rev. D **94**, 105006 (2016).
[40] D. Väänänen and G. C. McLaughlin, Uncovering the matter-neutrino resonance, Phys. Rev. D **93**, 105044 (2016).
[41] M. Frensel, M.-R. Wu, C. Volpe, and A. Perego, Neutrino flavor evolution in binary neutron star merger remnants, Phys. Rev. D **95**, 023011 (2017).
[42] J. Y. Tian, A. V. Patwardhan, and G. M. Fuller, Neutrino flavor evolution in neutron star mergers, Phys. Rev. D **96**, 043001 (2017).
[43] S. Shalgar, Multi-angle calculation of the matter-neutrino resonance near an accretion disk, J. Cosmol. Astropart. Phys. 02 (2018) 010.
[44] A. Vlasenko and G. C. McLaughlin, Matter-neutrino resonance in a multiangle neutrino bulb model, Phys. Rev. D **97**, 083011 (2018).
[45] I. Padilla-Gay, S. Shalgar, and I. Tamborra, Symmetry breaking due to multi-angle matter-neutrino resonance in neutron star merger remnants, arXiv:2403.15532.
[46] M.-R. Wu, M. George, C.-Y. Lin, and Z. Xiong, Collective fast neutrino flavor conversions in a 1D box: Initial conditions and long-term evolution, Phys. Rev. D **104**, 103003 (2021).
[47] S. Bhattacharyya and B. Dasgupta, Fast flavor depolarization of supernova neutrinos, Phys. Rev. Lett. **126**, 061302 (2021).
[48] S. Bhattacharyya and B. Dasgupta, Elaborating the ultimate fate of fast collective neutrino flavor oscillations, Phys. Rev. D **106**, 103039 (2022).
[49] S. Richers, H. Duan, M.-R. Wu, S. Bhattacharyya, M. Zaizen, M. George, C.-Y. Lin, and Z. Xiong, Code comparison for fast flavor instability simulations, Phys. Rev. D **106**, 043011 (2022).
[50] M. Zaizen and H. Nagakura, Simple method for determining asymptotic states of fast neutrino-flavor conversion, Phys. Rev. D **107**, 103022 (2023).
[51] M. Zaizen and H. Nagakura, Characterizing quasisteady states of fast neutrino-flavor conversion by stability and conservation laws, Phys. Rev. D **107**, 123021 (2023).
[52] Z. Xiong, M.-R. Wu, S. Abbar, S. Bhattacharyya, M. George, and C.-Y. Lin, Evaluating approximate asymptotic distributions for fast neutrino flavor conversions in a periodic 1D box, Phys. Rev. D **108**, 063003 (2023).
[53] H. Nagakura and M. Zaizen, Time-dependent and quasisteady features of fast neutrino-flavor conversion, Phys. Rev. Lett. **129**, 261101 (2022).
[54] H. Nagakura and M. Zaizen, Connecting small-scale to large-scale structures of fast neutrino-flavor conversion, Phys. Rev. D **107**, 063033 (2023).
[55] H. Duan and S. Shalgar, Flavor instabilities in the neutrino line model, Phys. Lett. B **747**, 139 (2015).
[56] S. Chakraborty, R. S. Hansen, I. Izaguirre, and G. G. Raffelt, Self-induced neutrino flavor conversion without flavor mixing, J. Cosmol. Astropart. Phys. 03 (2016) 042.
[57] F. Capozzi, B. Dasgupta, E. Lisi, A. Marrone, and A. Mirizzi, Fast flavor conversions of supernova neutrinos: Classifying instabilities via dispersion relations, Phys. Rev. D **96**, 043016 (2017).
[58] M. Chakraborty and S. Chakraborty, Three flavor neutrino conversions in supernovae: Slow & fast instabilities, J. Cosmol. Astropart. Phys. 01 (2020) 005.
[59] R. S. L. Hansen, S. Shalgar, and I. Tamborra, Enhancement or damping of fast neutrino flavor conversions due to collisions, Phys. Rev. D **105**, 123003 (2022).
[60] I. Tamborra, F. Hanke, H.-T. Janka, B. Müller, G. G. Raffelt, and A. Marek, Self-sustained asymmetry of lepton-number emission: A new phenomenon during the supernova shock-accretion phase in three dimensions, Astrophys. J. **792**, 96 (2014).
[61] R. Glas, H.-T. Janka, T. Melson, G. Stockinger, and O. Just, Effects of LESA in three-dimensional supernova simulations with multidimensional and ray-by-ray-plus neutrino transport, Astrophys. J. **881**, 36 (2019).
[62] J. Powell and B. Müller, Gravitational wave emission from 3D explosion models of core-collapse supernovae with low and normal explosion energies, Mon. Not. R. Astron. Soc. **487**, 1178 (2019).
[63] H. Nagakura, K. Sumiyoshi, and S. Yamada, Possible Early linear acceleration of proto-neutron stars via asymmetric neutrino emission in core-collapse supernovae, Astrophys. J. Lett. **880**, L28 (2019).